Modeling and Analysis of Parallel Mechanisms With Both Kinematic and Actuation Redundancies Via Screw Theory

Long Kang
Department of Electronic Systems Engineering,
Hanyang University,
Ansan 15588, Gyeonggi-do, South Korea
e-mail: hitjakie@gmail.com

Wheekuk Kim
Professor
Department of Electro-Mechanical System Engineering,
Korea University,
2511, Sejong-ro,
Sejong 339-700, South Korea
e-mail: wheekuk@korea.ac.kr

Byung-Ju Yi[1]
Professor
Department of Electronic Systems Engineering,
Hanyang University,
Ansan 15588, Gyeonggi-do, South Korea
e-mail: bj@hanyang.ac.kr

Two kinds of mechanical redundancies, namely kinematic redundancy and actuation redundancy, have been extensively studied due to their advantageous features in autonomous industry. Screw theory has been successfully applied to develop an analytical Jacobian of nonredundant parallel manipulators (PMs). However, to the best of our knowledge, screw theory has not been attempted for modeling of PMs with kinematic redundancies. Thus, first, through the mobility analysis of a simple nonredundant planar PM and its variations, this paper reviews kinematic and actuation redundancy systematically. Then, we demonstrated how to derive analytical Jacobian and also static force relationship for a PM with both kinematic and actuation redundancies by using the screw theory. Finally, simulations were performed to demonstrate the advantageous features of kinematic and actuation redundancies. [DOI: 10.1115/1.4037805]

Keywords: parallel mechanisms, theoretical kinematics, screw theory, kinematic redundancy, actuation redundancy

1 Introduction

Mobility of a system can be interpreted as the minimum number of independent variables which needs to be specified to locate its complete configuration. For a parallel manipulator (PM), when both the number of input actuators and dimension of the task space are equal to its mobility, we say that it is a nonredundant PM. Majority of nonredundant PMs suffer from some drawbacks such as small workspace due to type II singularities and meet difficulties in real-word applications due to the complexity of the unstructured environment, workspace obstacles, joint limits, and torque saturation due to the unexpected impact disturbance.

Aiming at utilizing the robot to execute complicated tasks in unstructured environments with high dexterity so as to realize high degree of autonomy, two kinds of redundancies, namely kinematic redundancy and actuation redundancy, have been proposed and extensively studied. Kinematic redundancy implies that the mobility of the manipulator is larger than the dimension of the task space. Kinematic redundancy can be utilized in applications of obstacle avoidance [1], singularity avoidance [2–4], satisfaction of some constraints including joint limits [5,6], minimize energy for specified task [7], increasing robustness [8] so as to improve reliability, increasing dexterity [9,10], etc. In addition, Yi et al. [11] used the kinematic redundancy to design a foldable parallel-type gripper which can be used to grasp irregular object. Later, Mohamed and Gosselin [12] highlighted the idea of using kinematic redundancy to design configurable Platforms of PMs. Recently, Isaksson et al. [13] utilized the kinematic redundancy to operate a gripper, which has the benefits of saving the cost of a gripper actuator and reducing the mass of the moving platform compared to most of the other PMs which can perform grasping task by an actuated gripping module attached to the moving platform directly. The actuation redundancy implies that the number of actuators is larger than the mobility of the manipulator. Actuation redundancies can be used to eliminate singularities [14,15], increase manipulability and stiffness [16,17], increase payload and acceleration [18] of the end-effector, improve the motion/force transmissibility [19] and yield an optimal load distribution [20] for more efficient design, avoid torque saturation, and admit fault tolerance [21] capability. Furthermore, for cable-driven robots, different force/load distribution algorithms [22–26] have been proposed by taking into account of the boundaries of the cable force or other constraints. These algorithms may also be applied to the load redistribution of redundantly actuated parallel mechanisms (actuated limbs are not cables) in a similar manner.

However, it should be noted that for redundantly actuated parallel mechanisms, it is hard to get a high positional accuracy by adopting the velocity control scheme, because velocities of active joints are dependent, and it has the risk of introducing excessive internal force and stress in the mechanism if the actuators are controlled independently. Hence, a small positional or modeling error may cause big internal force and stress, which can potentially break the mechanism.

Even though PMs with pure kinematic redundancy and actuation redundancy have been extensively studied, few researches have been found to combine them, namely design and analysis of PMs featuring with both kinematic and actuation redundancies. Human arm (shoulder, elbow, and wrist are generally modeled as seven degrees-of-freedom (7DOF) with 29 muscles) is a biological example which has both kinematic and actuation redundancies simultaneously in nature. Considering the advantageous features which could be introduced by kinematic and actuation redundancies, this paper aims to conduct modeling and analysis of PMs with both kinematic and actuation redundancies by using the screw theory.

As a fundamental to evaluate the performances (e.g., singularity, redundancy resolution, and manipulability) of PMs, velocity Jacobian is considered as a very important central issue in design and analysis of PMs. For nonredundant PMs, various approaches have been proposed to express the Jacobian. Among them, Davies method [27], closure-loop vector differentiation [4], and screw theory [28,29] are the three well-known methods. Davies method is an intuitive approach to build the input–output velocity relationship which can be used to formulate the Jacobian matrix by taking inverse of the matrix which relates the active joint velocities to passive joint velocities. The closure-loop vector differentiation is

[1]Corresponding author.

Manuscript received April 13, 2017; final manuscript received August 22, 2017; published online September 20, 2017. Assoc. Editor: Clement Gosselin.

a straightforward method commonly used in the literature. However, eliminating the passive joint velocity is usually complex especially when dealing with PMs with kinematic redundancy, making the derivation nontrivial.

Cox and Tesar [30,31] initially investigated kinematics of a spherical-type parallel mechanism with 3DOFs using the screw theory. The concept of reciprocal screw was applied to derive the analytical Jacobian. Mohammed and Duffy [28] investigated the analytical Jacobian for fully parallel PMs using the concept of reciprocal screws. Specifically, reciprocal screw was found very effective to obtain the analytical Jacobian of lower-mobility PMs [29,32,33]. More recently, making use of the reciprocal screw in the screw theory has been popular in the modeling of both serial manipulators and nonredundant PMs. Compared with the first two methods, screw-based method is more efficient and provides a deeper insight into the constraint and actuation wrenches of the robotic system. Moreover, the screw-based Jacobian could be more powerful and intuitive (by using line geometry) in singularity analysis. However, to the best of our knowledge, the screw-based method has not been attempted for the analysis of the PMs with kinematic redundancy. In this paper, we will present how to extend the traditional screw-based method to derive the Jacobian of PMs with kinematic redundancy and PMs with both kinematic and actuation redundancies for the first time. We believe that this small progress will outline a complete graph of Jacobian analysis of general PMs by using the screw theory. However, we have to mention that for screw-based singularity analysis, checking the actuation wrench is sufficient, and the Jacobian is not always required [34,35].

In order to achieve and illustrate the goals we mentioned before, we first start from modeling and analysis of a simple nonredundant 3-RRR PM, and then extend it to the kinematically redundant 3-$\overline{\text{R}}$PRR PM and redundantly actuated 4-RRR PM. Finally, we move to the 3-RPRR PM which has both kinematic and actuation redundancies. Finally, some simulations are performed to demonstrate the advantages of kinematic and actuation redundancies.

2 Mobility and Redundancy

2.1 Mobility. Mobility implies the minimum number of input required for describing the whole system. Gogu [36] reviewed more than 35 contributions on calculation of the mobility critically by investigating their genesis, similarities, and limitations. Among them, the well-known Grübler–Kutzbach criterion is one of the most commonly used approaches for the mobility calculation of a PM without redundant constraints. Unfortunately, the obtained mobility from this criterion does not show the motion property of the PM since it does not take into account the overconstraints of the PMs. With the help of reciprocal screw, Li and Huang [37] have modified this criterion by taking the common constraints and passive constraints into consideration. Later, Dai et al. [38] revealed this process and combined the motion and constraint screw systems to build a modified Grübler–Kutzbach criterion, which evaluates the mobility of over-constrained PMs correctly, as shown below:

$$M = d(n - g - 1) + \sum_{i=1}^{g} f_i + \upsilon \tag{1}$$

By using the number of independent loops, an alternative form can be written as

$$M = \sum_{i=1}^{g} f_i - dl + \upsilon \tag{2}$$

where M denotes the mobility of the mechanism; d is the dimension of the mechanism joint motion screw system that spans the feasible motion space of all limbs of the mechanism; n is the number of links including the ground; g is the number of joints; f_i is the DOF of the joint i; l is the number of independent loops; υ is the number of redundant constraint screws. It is noted that $d = 6 - \lambda$, where λ denotes the number of common constraint screws, which are imposed on the common moving platform by each limb.

2.2 Redundancy. As we mentioned above, mechanical redundancy can be classified into kinematic redundancy and actuation redundancy as shown in Table 1.

Let M denote the mobility of the system, and N denote the dimension of the task space. Kinematic redundancy is a relative concept which holds with respect to a given task. Kinematic redundancy implies that the PMs has more DOFs than strictly required for executing certain task, namely $M > N$. In general, kinematic redundancies can be classified into two categories:

- Only partial DOFs of the end-effector is utilized to execute some certain task (task redundancy [39]). For example, a 6DOF robot used for arc welding tasks which requires only 5DOFs is functionally redundant, and this task leaves an extra DOF in the operational space which can be exploited to achieve other objectives such as joint-limit/singularity/obstacle avoidance.
- The joint twists in at least one kinematic chain are dependent to each other, which implies that there exists joint redundancy, and self-motion is allowed in this kinematic chain. (Redundancy happens in the kinematic chain, and dimension of the joint space in this kinematic chain is greater than the output dimension of this serial chain.)

Moreover, let N_{ta} denotes the number of active joints. Actuation redundancy implies that the PM has more actuators than strictly required to locate configuration of the robot system, namely $N_{ta} > M$. In general, actuation redundancy can be classified into two categories

- Passive joints in kinematic chains are actuated. Disadvantages of this approach are increased mass and inertia due to the additional floating actuators.
- Adding additional actuated kinematic chains to the system. Disadvantages of this approach are reduction of the workspace and dexterity.

For actuation redundancy, besides independent inputs in PMs as many as the mobility, there exist many potential input locations where additional actuators can be placed. Those additional inputs can be utilized to load distribution for maximizing payload, minimizing torque saturation of actuators, etc. By considering actuator limits, the wrench that could be sustained by a manipulator for a given posture can be maximized [40]. Another advantage of using redundant actuation is to balance the PM using antagonistic actuation, which corresponds to null-space operation of kinematically redundant manipulators.

3 Kinematic Modeling

A simple nonredundant 3-RRR planar PM [41,42] and its variations are used to demonstrate the difference between the nonredundant PMs, PMs with kinematic redundancy, and PMs with both kinematic and actuation redundancies through their mobility and redundancy analysis, Jacobian derivation, and static force relationship. For each type, mobility analysis, Jacobian formulation, and static force relationship will be performed by using the screw theory. Especially, we will show how to build the Jacobian of PMs with kinematic redundancy by using the screw theory for the first time and also reveal the intrinsic property of PMs with both kinematic and actuation redundancies.

First, summary of the Jacobian model for the PM with nonredundancy, kinematic redundancy, actuation redundancy, and with

Table 1 Redundancy classification

Redundancy classification	Condition	Realizing methodology
Kinematic redundancy	$M > N$	Partial DOFs of the end-effector are selected as the task space Joint twists in at least one kinematic chain are dependent
Actuation redundancy	$N_{ta} > M$	Passive joints are actuated Adding additional actuated kinematic chains

M, mobility; N, dimension of the task space; N_{ta}, number of actuators

both kinematic and actuation redundancies by using the screw theory is given as below:

$$\boldsymbol{A}\dot{\mathbf{u}} = \boldsymbol{B}\dot{\boldsymbol{\theta}},\ \ \boldsymbol{A} \in R^{P\times N},\ \ \boldsymbol{B} \in R^{P\times N_{ta}} \tag{3}$$

where $\boldsymbol{A}$ and $\boldsymbol{B}$ are built with actuation wrenches and active joint twists (screw theory).

M is the mobility; N_{ta} is the number of actuators; N is the dimension of the task space; P is the number of actuation wrenches.

Then, it can be concluded that with respect to the mobility M
when $M > N$: kinematic redundancy
when $N_{ta} > M$: actuation redundancy
when $N_{ta} < M$: underactuated system
when $N_{ta} > M > N$: kinematic and actuation redundancies
when $N_{ta} = M = N$, nonredundant system.

Moreover, by comparing with the actuation wrenches (P), we have
when $P > N$: actuation redundancy
when $P = N$: no actuation redundancy
when $P < N$: underactuated system.

Furthermore, we have to mention that in general matrices $\boldsymbol{A}$ and $\boldsymbol{B}$ are not unique due to the fact that different methods can be applied to obtain this kind of kinematic/force transmission relationship. As far as the screw-based method is concerned, selection of the independent actuation wrench may also have several choices, namely elements of these two matrices may not be unique. However, dimension of them would be unique for kinematic/force redundancy analysis.

Moreover, these categories only consider the conventional parallel mechanisms which can be fully controlled (actuated). For special topology of parallel mechanisms (e.g., 2-RRR PM where the axis of the end joint in each chain coincides, one unconstrained tool rotation exists), they should be analyzed case by case in terms of both Jacobian and singularity analysis.

3.1 Jacobian of the Nonredundant 3-RRR PM. Schematic diagram of the 3-RRR (type) PM is shown in Fig. 1, where the underlined letter denotes an active joint. With respect to the moving coordinate frame ($P - X_tY_tZ_t$), joint twists of limb i can be found as

$$\begin{aligned}
\$_{i1} &= \begin{pmatrix} \hat{z} & (\mathbf{PC}_i + \mathbf{C}_i\mathbf{B}_i + \mathbf{B}_i\mathbf{A}_i) \times \hat{z} \end{pmatrix} \\
\$_{i2} &= \begin{pmatrix} \hat{z} & (\mathbf{PC}_i + \mathbf{C}_i\mathbf{B}_i) \times \hat{z} \end{pmatrix} \\
\$_{i3} &= \begin{pmatrix} \hat{z} & \mathbf{PC}_i \times \hat{z} \end{pmatrix}
\end{aligned} \tag{4}$$

Then, the constraint wrenches of each limb can be found as

$$\begin{aligned}
\$^c_{i1} &= \begin{pmatrix} 0 & \hat{x} \end{pmatrix} \\
\$^c_{i2} &= \begin{pmatrix} 0 & \hat{y} \end{pmatrix} \\
\$^c_{i3} &= \begin{pmatrix} \hat{z} & 0 \end{pmatrix}
\end{aligned} \tag{5}$$

Based on the mobility calculation formula in Eq. (1), the above three identical constraint wrenches provided by each limb is considered as the common constraint wrenches imposed to the moving platform. Thus, the number of common constraint screws of each limb is three. Excluded these three common constraint wrenches in each limb, no other constraint wrenches exist. Hence, redundant constraint wrenches also not exist

$$\lambda = 3,\ \upsilon = 0 \tag{6}$$

Using Eq. (1), we have

$$M = (6-3)(8-9-1) + 9 + 0 = 3 \tag{7}$$

By finding the motion-screws of this PM which are reciprocal to the common constraints in Eq. (5), we know that this planar 3-RRR PM has 3DOFs, namely two translational DOFs in the plane and one rotational DOF about the axis perpendicular to this plane.

In the following, the first and second subscripts given in general $(\cdot)_{ij}$ denote the limb number and the joint number of the limb, respectively. If the first joint of each limb is selected as the active joint $\left(\boldsymbol{\theta}_a = \begin{pmatrix}\theta_{11} & \theta_{21} & \theta_{31}\end{pmatrix}^{\mathrm{T}}\right)$, and the task space is chosen as the whole planar motion $\left(\text{i.e., } \boldsymbol{u} = \begin{pmatrix} x & y & \phi_z \end{pmatrix}^{\mathrm{T}}\right)$, then no redundancy exists ($M=3, N=3, N_{ta}=3$).

In the previous work [29,43], each actuation wrench is defined as the wrench which is reciprocal to all the joint twists of each limb except for the active joint twist. Actuation wrench of each limb can be found as

$$\$^r_{i1} = \begin{pmatrix} \mathbf{B}_i\mathbf{C}_i & \mathbf{PC}_i \times \mathbf{B}_i\mathbf{C}_i \end{pmatrix} \tag{8}$$

where $\$^r_{i1} \circ \$_{i1} \neq 0$. Its physical meaning can be interpreted as the wrench of actuation imposed by the first joint of the ith limb on the end-effector and can only generate virtual work on the corresponding active joint twist.

Output motion twist of the end-effector can be expressed in terms of joint twists of each chain as below:

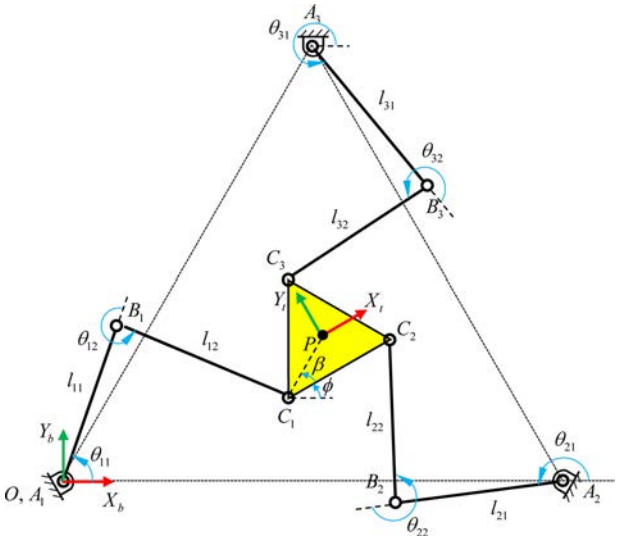

Fig. 1 Schematic diagram of the 3-RRR nonredundant manipulator

$$\$_P = \begin{pmatrix} \boldsymbol{\omega} \\ \boldsymbol{v} \end{pmatrix} = \sum_{j=1}^{3} \dot{\theta}_{ij} \$_{ij} = \dot{\theta}_{i1} \$_{i1} + \dot{\theta}_{i2} \$_{i2} + \dot{\theta}_{i1} \$_{i3} \quad (i = 1...3) \tag{9}$$

For each limb, taking the orthogonal product "$\circ$" of both sides of Eq. (9) with the corresponding actuation wrench in Eq. (8), yields

$$\$^r_{i1} \circ \$_P = \$^r_{i1} \circ \$_{i1} \dot{\theta}_{i1} \quad (i = 1...3) \tag{10}$$

Writing Eq. (10) in matrix form as

$$\boldsymbol{A}\dot{\boldsymbol{u}} = \boldsymbol{B}\dot{\boldsymbol{\theta}}_a \tag{11}$$

where

$$\begin{aligned} \boldsymbol{A} &= \begin{bmatrix} \mathbf{B}_1\mathbf{C}_1 & \hat{z} \cdot (\mathbf{PC}_1 \times \mathbf{B}_1\mathbf{C}_1) \\ \mathbf{B}_2\mathbf{C}_2 & \hat{z} \cdot (\mathbf{PC}_2 \times \mathbf{B}_2\mathbf{C}_3) \\ \mathbf{B}_3\mathbf{C}_3 & \hat{z} \cdot (\mathbf{PC}_3 \times \mathbf{B}_3\mathbf{C}_3) \end{bmatrix} \in R^{3\times3} \\ \boldsymbol{B} &= \mathrm{diag}(\$^r_{i1} \circ \$_{i1}) \in R^{3\times3} \quad (i = 1...3) \\ \dot{\boldsymbol{u}} &= \begin{pmatrix} v_x & v_y & w_z \end{pmatrix}^T, \ \dot{\boldsymbol{\theta}}_a = \begin{pmatrix} \dot{\theta}_{11} & \dot{\theta}_{21} & \dot{\theta}_{31} \end{pmatrix}^{\mathrm{T}} \end{aligned} \tag{12}$$

The overall forward Jacobian matrix can be expressed as

$$\boldsymbol{J} = \boldsymbol{A}^{-1}\boldsymbol{B} \tag{13}$$

The dual static force relationship can be given by

$$\boldsymbol{\tau}_a = \boldsymbol{J}^{\mathrm{T}}\boldsymbol{F} \tag{14}$$

where $\boldsymbol{\tau}_a = \begin{pmatrix} \tau_{11} & \tau_{21} & \tau_{31} \end{pmatrix}^{\mathrm{T}}$.

3.2 Jacobian of the 3-RPRR PM With Kinematic Redundancy. By adding one additional active prismatic joint to each limb of 3-RRR, a kinematically redundant 3-RPRR PM [44] can be obtained as shown in Fig. 2. Joint twists of limb i can be found as

$$\begin{aligned} \$_{i1} &= \begin{pmatrix} \hat{z} & (\mathbf{PC}_i + \mathbf{C}_i\mathbf{B}_i + \mathbf{B}_i\mathbf{A}_i) \times \hat{z} \end{pmatrix} \\ \$_{i2} &= \begin{pmatrix} 0 & \widehat{\mathbf{A}_i\mathbf{B}_i} \end{pmatrix} \\ \$_{i3} &= \begin{pmatrix} \hat{z} & (\mathbf{PC}_i + \mathbf{C}_i\mathbf{B}_i) \times \hat{z} \end{pmatrix} \\ \$_{i4} &= \begin{pmatrix} \hat{z} & \mathbf{PC}_i \times \hat{z} \end{pmatrix} \end{aligned} \tag{15}$$

Constraint wrenches of each limb can be found the same as Eq. (5). Thus, Eq. (6) still holds for this PM. Using Eq. (1), mobility of this manipulator can be found as

$$M = (6-3)(11-12-1) + 12 + 0 = 6 \tag{16}$$

Compared with the 3-RRR PM, three more DOFs are increased due to fact that the four joint twists in each limb are dependent to each other and the degree of dependency is one. There exists infinite number of inverse kinematic solutions for the specified output $\boldsymbol{u} = \begin{pmatrix} x & y & \phi_z \end{pmatrix}^{\mathrm{T}}$ in the task space. Due to the fact that $M = 6$, $N = 3$, $N_{la} = 6$, the degree of kinematic redundancies of this 3-RPRR PM is three.

Previous work on Jacobian derivation of PMs by using screw theory was based on the assumption that the PM has no kinematic redundancy, where you can find the actuation wrench associated with each active joint, respectively. In this work, we rename this kind of actuation wrench to the "pure actuation wrench," because each of them can only generate virtual work on its corresponding active joint. However, no research works have been found to apply the screw theory to build Jacobian of PMs with kinematic redundancy to the best of our knowledge. For the given example of 3-RPRR PM with kinematic redundancy, there exist two active joints in each limb. If you stick to using the rule of Jacobian derivation developed for nonredundant PMs, you should find two pure actuation wrenches associated with the two active joints, respectively. However, there does not exist two pure actuation wrenches for this kind of PMs with kinematic redundancy. This concept has not been mentioned in the previous research. And maybe because of this, nobody has ever tried to use the screw theory to build Jacobian of PMs with kinematic redundancy. Here, in this paper, we will try to clear this concept and use the screw theory to develop the Jacobian of PMs with kinematic redundancy for the first time.

Mathematically in order to eliminate power created by the passive joint velocity in the formulation of the output motion twist, we should find the actuation wrench which is reciprocal to all the passive joint twists of each limb. Due to the fact that each limb of the 3-RPRR PM has two passive joints, dimension of the reciprocal screws system is four. Obviously, this reciprocal screw system includes the three independent constraint wrenches of this PM. Hence, only one reciprocal basis screw which does not belong to the constraint wrench system can be found as the actuation wrench for each limb. We name this kind of actuation wrench to the "general actuation wrench" in contrast to the "pure actuation wrench" existed in nonredundant PMs. It can be found that the number of actuation wrenches is different from the number of active joints in redundant limb. Due to the fact that joint twists in limbs of PMs with kinematic redundancy are dependent to each other, the general actuation wrench obtained may generate virtual work on more than one active joint, while the pure actuation wrench in nonredundant PMs can only generate work on the corresponding active joint.

Based on the previous analysis, the general actuation wrench of each limb for the kinematically redundant 3-RPRR PM in Fig. 2 can be found as

$$\$^r_{i\_12} = \begin{pmatrix} \mathbf{B}_i\mathbf{C}_i & \mathbf{PC}_i \times \mathbf{B}_i\mathbf{C}_i \end{pmatrix} \tag{17}$$

where $\$^r_{i\_12} \circ \$_{i1} \neq 0$, $\$^r_{i\_12} \circ \$_{i2} \neq 0$ may be satisfied simultaneously. It is noted that this actuation wrench does not create any power on the two passive joints of each limb. On the other hand, this actuation wrench does create power on the two active joints of each limb.

Output motion twist of the end-effector can be expressed in terms of joint twists of each limb as

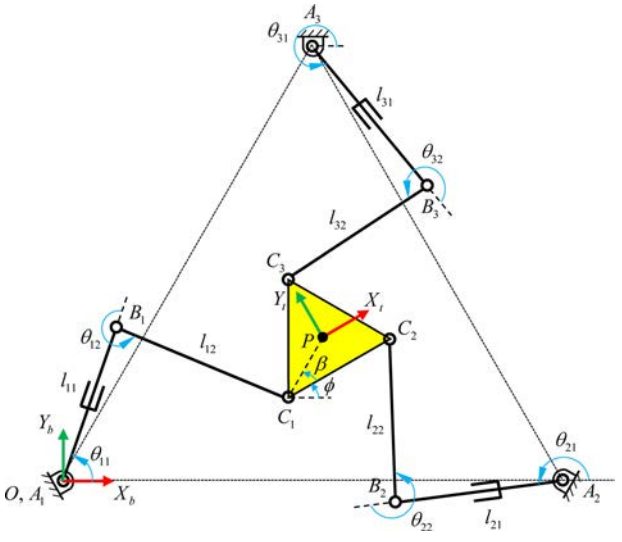

Fig. 2 Schematic diagram of the 3-RPRR kinematically redundant manipulator

$$\$_P = \begin{pmatrix} \boldsymbol{\omega} \\ \boldsymbol{v} \end{pmatrix} = \sum_{j=1}^{3} \dot{\theta}_{ij} \$_{ij}$$
$$= \dot{\theta}_{i1} \$_{i1} + \dot{l}_{i1} \$_{i2} + \dot{\theta}_{i2} \$_{i3} + \dot{\theta}_{i3} \$_{i4} \ (i = 1...3) \tag{18}$$

For each limb, taking the orthogonal product of both sides of Eq. (18) with the general actuation wrench in Eq. (17), yields

$$\$^r_{i\_12} \circ \$_P = \$^r_{i\_12} \circ \$_{i1} \dot{\theta}_{i1} + \$^r_{i\_12} \circ \$_{i2} \dot{l}_{i1} \quad (i = 1...3) \tag{19}$$

Writing Eq. (19) in matrix form as

$$\boldsymbol{A}\dot{\boldsymbol{u}} = \boldsymbol{B}\dot{\boldsymbol{\theta}}_a \tag{20}$$

where

$$\boldsymbol{A} = \begin{bmatrix} \mathbf{B}_1\mathbf{C}_1 & \hat{z} \cdot (\mathbf{PC}_1 \times \mathbf{B}_1\mathbf{C}_1) \\ \mathbf{B}_2\mathbf{C}_2 & \hat{z} \cdot (\mathbf{PC}_2 \times \mathbf{B}_2\mathbf{C}_2) \\ \mathbf{B}_3\mathbf{C}_3 & \hat{z} \cdot (\mathbf{PC}_3 \times \mathbf{B}_3\mathbf{C}_3) \end{bmatrix} \in R^{3\times3},$$
$$\boldsymbol{B} = \begin{bmatrix} \xi_1 & \lambda_1 & 0 & 0 & 0 & 0 \\ 0 & 0 & \xi_2 & \lambda_2 & 0 & 0 \\ 0 & 0 & 0 & 0 & \xi_3 & \lambda_3 \end{bmatrix} \in R^{3\times6}$$
$$\xi_i = \$^r_{i\_12} \circ \$_{i1}, \quad \lambda_i = \$^r_{i\_12} \circ \$_{i2}$$
$$\dot{\boldsymbol{u}} = \begin{pmatrix} v_x & v_y & w_z \end{pmatrix}^{\mathrm{T}}, \quad \dot{\boldsymbol{\theta}}_a = \begin{pmatrix} \dot{\theta}_{11} & \dot{l}_{11} & \dot{\theta}_{21} & \dot{l}_{21} & \dot{\theta}_{31} & \dot{l}_{31} \end{pmatrix}^{\mathrm{T}} \tag{21}$$

The forward kinematics of the PM with kinematic redundancy can be expressed as

$$\dot{\boldsymbol{u}} = \boldsymbol{J}\dot{\boldsymbol{\theta}}_a \tag{22}$$

where $\boldsymbol{J} = \boldsymbol{A}^{-1}\boldsymbol{B}$.

The general inverse kinematic solutions at velocity level can be obtained as

$$\dot{\boldsymbol{\theta}}_a = \boldsymbol{J}^{\mathrm{T}}(\boldsymbol{J}\boldsymbol{J}^{\mathrm{T}})^{-1}\dot{\boldsymbol{u}} + \left(\boldsymbol{I} - \boldsymbol{J}^{\mathrm{T}}(\boldsymbol{J}\boldsymbol{J}^{\mathrm{T}})^{-1}\boldsymbol{J}\right)\boldsymbol{\varepsilon} \tag{23}$$

where $\boldsymbol{I} \in R^{6\times6}$ is an identity matrix. $\boldsymbol{\varepsilon} \in R^6$ is an arbitrary vector which depends on secondary criteria to be optimized. The first term of Eq. (23) represents the minimum-norm solution, and the second term represents the null space solution.

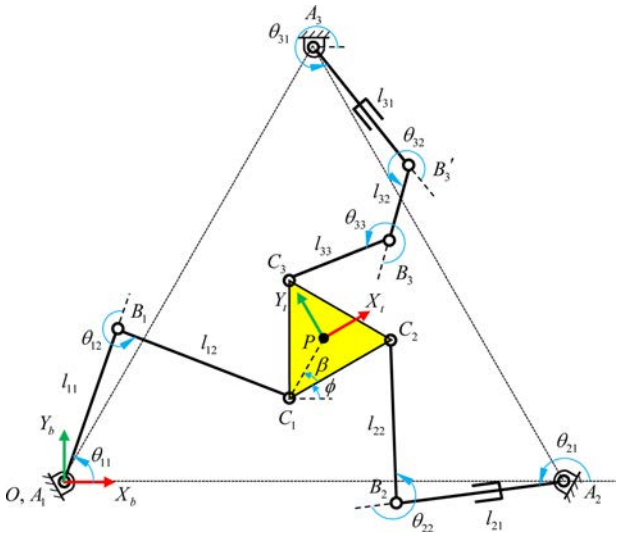

Fig. 3 Schematic diagram of the RRR-RPRR-RPRRR kinematically redundant manipulator

And general inverse kinematic solutions of the following example PMs with kinematic redundancies can be found in the same way.

The static force relationship can be given by

$$\boldsymbol{\tau}_a = \boldsymbol{J}^{\mathrm{T}}\boldsymbol{F} \tag{24}$$

where $\boldsymbol{\tau}_a = \begin{pmatrix} \tau_{11} & f_{11} & \tau_{21} & f_{21} & \tau_{31} & f_{31} \end{pmatrix}^{\mathrm{T}}$.

3.3 Jacobian of the RRR-RPRR-RPRRR PM With Kinematic Redundancy. In order to illustrate the method proposed above in a more general sense, we apply our methodology to another kinematically redundant PM with asymmetric structure to show how to develop its Jacobian matrix. As depicted in Fig. 3, the PM under study is a RRR-RPRR-RPRRR planar PM, which has three asymmetric limbs and each limb has different number of actuators. The first and second limb structures (RRR and RPRR) have been discussed in the above two examples. Thus, their joint twists, constraint and actuation wrenches should share the same form as before, which will not be discussed any more here. For the third limb, joint twists can be written as

$$\begin{aligned} \$_{31} &= \begin{pmatrix} \hat{z} & (\mathbf{PC}_3 + \mathbf{C}_3\mathbf{B}_3 + \mathbf{B}_3\mathbf{B}_3' + \mathbf{B}_3'\mathbf{A}_3) \times \hat{z} \end{pmatrix} \\ \$_{32} &= \begin{pmatrix} 0 & \widehat{\mathbf{A}_3\mathbf{B}_3'} \end{pmatrix} \\ \$_{33} &= \begin{pmatrix} \hat{z} & (\boldsymbol{PC}_3 + \mathbf{C}_3\mathbf{B}_3 + \mathbf{B}_3\mathbf{B}_3') \times \hat{z} \end{pmatrix} \\ \$_{34} &= \begin{pmatrix} \hat{z} & (\mathbf{PC}_3 + \mathbf{C}_3\mathbf{B}_3) \times \hat{z} \end{pmatrix} \\ \$_{35} &= \begin{pmatrix} \hat{z} & \mathbf{PC}_3 \times \hat{z} \end{pmatrix} \end{aligned} \tag{25}$$

Constraint wrenches of this limb can be found the same as Eq. (5). Thus, mobility of this PM can be found through the same formula as Eq. (16). With respect to the three-dimensional planar task space at the end-effector, this PM has three degrees of kinematic redundancies ($M = 6$, $N = 3$, $N_{ta} = 6$), where the redundancies represent the allowed self-motions in second and third limbs. Even though the third limb has three active joints, only one general actuation wrench can be found due to that there exist two passive joints in this limb. The only general actuation wrench can be given as

$$\$^r_{3\_123} = \begin{pmatrix} \mathbf{B}_3\mathbf{C}_3 & \mathbf{PC}_1 \times \mathbf{B}_3\mathbf{C}_3 \end{pmatrix} \tag{26}$$

where $\$^r{}_{3\_123} \circ \$_{31} \neq 0$, $\$^r{}_{3\_123} \circ \$_{32} \neq 0$, $\$^r{}_{3\_123} \circ \$_{33} \neq 0$ may be satisfied simultaneously. Output motion twist can be expressed in terms of each limb as

$$\begin{aligned} \$_P &= \begin{pmatrix} \boldsymbol{\omega} \\ \boldsymbol{v} \end{pmatrix} \\ &= \dot{\theta}_{11}\$_{11} + \dot{\theta}_{12}\$_{12} + \dot{\theta}_{11}\$_{13} \\ &= \dot{\theta}_{21}\$_{21} + \dot{l}_{21}\$_{22} + \dot{\theta}_{22}\$_{23} + \dot{\theta}_{23}\$_{24} \\ &= \dot{\theta}_{31}\$_{31} + \dot{l}_{31}\$_{32} + \dot{\theta}_{32}\$_{33} + \dot{\theta}_{33}\$_{34} + \dot{\theta}_{34}\$_{35} \end{aligned} \tag{27}$$

For the third limb, takin the orthogonal product of both sides of Eq. (27) with its corresponding actuation wrench in Eq. (26), yields

$$\$^r_{3\_123} \circ \$_P = \$^r_{3\_123} \circ \$_{31}\dot{\theta}_{31} + \$^r_{3\_123} \circ \$_{32}\dot{l}_{31} + \$^r_{3\_123} \circ \$_{33}\dot{\theta}_{32} \tag{28}$$

Combining Eqs. (10) and (19) with Eq. (28), and writing them in matrix form as

$$\boldsymbol{A}\dot{\boldsymbol{u}} = \boldsymbol{B}\dot{\theta}_a \tag{29}$$

where

$$\boldsymbol{A} = \begin{bmatrix} \mathbf{B}_1\mathbf{C}_1 & \hat{z}\cdot(\mathbf{PC}_1 \times \mathbf{B}_1\mathbf{C}_1) \\ \mathbf{B}_2\mathbf{C}_2 & \hat{z}\cdot(\mathbf{PC}_2 \times \mathbf{B}_2\mathbf{C}_2) \\ \mathbf{B}_3\mathbf{C}_3 & \hat{z}\cdot(\mathbf{PC}_3 \times \mathbf{B}_3\mathbf{C}_3) \end{bmatrix} \in R^{3\times 3},$$

$$\boldsymbol{B} = \begin{bmatrix} \xi_1 & 0 & 0 & 0 & 0 & 0 \\ 0 & \xi_2 & \lambda_2 & 0 & 0 & 0 \\ 0 & 0 & 0 & \xi_3 & \lambda_3 & \beta_3 \end{bmatrix} \in R^{3\times 6}$$

$$\xi_1 = \boldsymbol{\$}^r{}_{11} \circ \boldsymbol{\$}_{11}$$

$$\xi_2 = \boldsymbol{\$}^r{}_{2\_12} \circ \boldsymbol{\$}_{21}, \quad \lambda_2 = \boldsymbol{\$}^r{}_{2\_12} \circ \boldsymbol{\$}_{22}$$

$$\xi_3 = \boldsymbol{\$}^r{}_{3\_123} \circ \boldsymbol{\$}_{31}, \quad \lambda_3 = \boldsymbol{\$}^r{}_{3\_123} \circ \boldsymbol{\$}_{32}, \quad \beta_3 = \boldsymbol{\$}^r{}_{3\_123} \circ \boldsymbol{\$}_{33}$$

$$\dot{\boldsymbol{u}} = \begin{pmatrix} v_x & v_y & w_z \end{pmatrix}^{\mathrm{T}}, \quad \dot{\boldsymbol{\theta}}_a = \begin{pmatrix} \dot{\theta}_{11} & \dot{\theta}_{21} & \dot{l}_{21} & \dot{\theta}_{31} & \dot{l}_{31} & \dot{\theta}_{32} \end{pmatrix}^{\mathrm{T}} \tag{30}$$

The overall forward Jacobian matrix can be expressed as

$$\boldsymbol{J} = \boldsymbol{A}^{-1}\boldsymbol{B} \tag{31}$$

The static force relationship can be given by

$$\boldsymbol{\tau}_a = \boldsymbol{J}^{\mathrm{T}}\boldsymbol{F} \tag{32}$$

where $\boldsymbol{\tau}_a = \begin{pmatrix} \tau_{11} & \tau_{21} & f_{21} & \tau_{31} & f_{31} & \tau_{32} \end{pmatrix}^{\mathrm{T}}$.

3.4 Jacobian of the 4-RRR PM With Actuation Redundancy. By adding one additional actuated kinematic chain RRR to the nonredundant 3-RRR PM, a redundantly actuated 4-RRR PM as shown in Fig. 4 can be obtained. This PM has one degree of actuation redundancies due to the fact that $M = 3$, $N = 3$, $N_{ta} = 4$. All of the four limbs share the same limb structure as the 3-RRR PM. Thus, their joint twists, constraint, and actuation wrenches should share the same form as before, which will not be discussed any more here. Output motion twist of the end-effector can be expressed in terms of joint twists of each chain as below:

$$\boldsymbol{\$}_P = \begin{pmatrix} \boldsymbol{\omega} \\ \boldsymbol{v} \end{pmatrix} = \sum_{j=1}^{3} \dot{\theta}_{ij}\boldsymbol{\$}_{ij} = \dot{\theta}_{i1}\boldsymbol{\$}_{i1} + \dot{\theta}_{i2}\boldsymbol{\$}_{i2} + \dot{\theta}_{i1}\boldsymbol{\$}_{i3} \; (i = 1\ldots4) \tag{33}$$

For each limb, taking the orthogonal product "$\circ$" of both sides of Eq. (33) with its corresponding actuation wrench of Eq. (8), yields

$$\boldsymbol{\$}^r{}_{i1} \circ \boldsymbol{\$}_P = \boldsymbol{\$}^r{}_{i1} \circ \boldsymbol{\$}_{i1}\dot{\theta}_{i1} \quad (i = 1\ldots4) \tag{34}$$

Writing Eq. (34) in matrix form as

$$\mathbf{A}\dot{\mathbf{u}} = \boldsymbol{B}\dot{\boldsymbol{\theta}}_a \tag{35}$$

where

$$\boldsymbol{A} = \begin{bmatrix} \mathbf{B}_1\mathbf{C}_1 & \hat{z}\cdot(\mathbf{PC}_1 \times \mathbf{B}_1\mathbf{C}_1) \\ \mathbf{B}_2\mathbf{C}_2 & \hat{z}\cdot(\mathbf{PC}_2 \times \mathbf{B}_2\mathbf{C}_2) \\ \mathbf{B}_3\mathbf{C}_3 & \hat{z}\cdot(\mathbf{PC}_3 \times \mathbf{B}_3\mathbf{C}_3) \\ \mathbf{B}_4\mathbf{C}_4 & \hat{z}\cdot(\mathbf{PC}_4 \times \mathbf{B}_4\mathbf{C}_4) \end{bmatrix} \in R^{4\times 3} \tag{36}$$

$$\boldsymbol{B} = \mathrm{diag}(\boldsymbol{\$}^r{}_{i1} \circ \boldsymbol{\$}_{i1}) \in R^{4\times 4} \quad (i = 1\ldots4)$$

$$\dot{\boldsymbol{u}} = \begin{pmatrix} v_x & v_y & w_z \end{pmatrix}^{\mathrm{T}}, \quad \dot{\boldsymbol{\theta}}_a = \begin{pmatrix} \dot{\theta}_{11} & \dot{\theta}_{21} & \dot{\theta}_{31} & \dot{\theta}_{41} \end{pmatrix}^{\mathrm{T}}$$

The overall inverse Jacobian matrix can be expressed as

$$\boldsymbol{J} = \boldsymbol{B}^{-1}\boldsymbol{A} \tag{37}$$

The dual static force relationship can be given by

$$\boldsymbol{F} = \boldsymbol{J}^{\mathrm{T}}\boldsymbol{\tau}_a \tag{38}$$

where $\boldsymbol{\tau}_a = \begin{pmatrix} \tau_{11} & \tau_{21} & \tau_{31} & \tau_{41} \end{pmatrix}^{\mathrm{T}}$.

The general solution of Eq. (38) can be given as

$$\boldsymbol{\tau}_a = (\boldsymbol{J}^{\mathrm{T}})^{+}\boldsymbol{F} + \left(\boldsymbol{I} - (\boldsymbol{J}^{\mathrm{T}})^{+}\boldsymbol{J}^{\mathrm{T}}\right)\boldsymbol{\varepsilon} \tag{39}$$

where $(\boldsymbol{J}^{\mathrm{T}})^{+} = \boldsymbol{J}(\boldsymbol{J}^{\mathrm{T}}\boldsymbol{J})^{-1} \in R^{4\times 3}$, $\boldsymbol{I} \in R^{4\times 4}$ is an identity matrix, and $\boldsymbol{\varepsilon} \in R^4$ is an arbitrary vector.

3.5 Jacobian of the 3-RPRR PM With Both Kinematic and Actuation Redundancies. A PM with both kinematic and actuation redundancies can be obtained by adding additional actuators on passive joints in each limb of the kinematically redundant 3-RPRR PM shown in Fig. 2. Specifically, we will consider the case of 3-RPRR PM in which the first passive joint of each limb is additionally activated. This PM has both kinematic and actuation redundancies due to the fact that $M = 6$, $N = 3$, $N_{ta} = 9$. As there exists only one passive joint in each limb, the number of independent general actuation wrenches in each limb should be two according to the above discussion. Each of them may generate virtual work on not only one active joint. Here, two independent actuation wrenches can be selected as

$$\boldsymbol{\$}^r{}_{i\_12} = \begin{pmatrix} \mathbf{B}_i\mathbf{C}_i & \mathbf{PC}_i \times \mathbf{B}_i\mathbf{C}_i \end{pmatrix} \tag{40}$$

$$\boldsymbol{\$}^r{}_{i\_123} = \begin{pmatrix} \mathbf{B}_i\mathbf{C}_i^{\perp} & \mathbf{PC}_i \times \mathbf{B}_i\mathbf{C}_i^{\perp} \end{pmatrix} \tag{41}$$

where

$$\boldsymbol{\$}^r{}_{i\_12} \circ \boldsymbol{\$}_{i1} \neq 0, \quad \boldsymbol{\$}^r{}_{i\_12} \circ \boldsymbol{\$}_{i2} \neq 0$$

$$\boldsymbol{\$}^r{}_{i\_123} \circ \boldsymbol{\$}_{i1} \neq 0, \quad \boldsymbol{\$}^r{}_{i\_123} \circ \boldsymbol{\$}_{i2} \neq 0, \quad \boldsymbol{\$}^r{}_{i\_123} \circ \boldsymbol{\$}_{i3} \neq 0$$

And $\boldsymbol{B_iC_i}^{\perp}$ represents a line (lies in the plane) passing through point c_i and perpendicular to the line $\boldsymbol{B_iC_i}$. However, we have to mention that selection of two independent actuation wrenches is not unique.

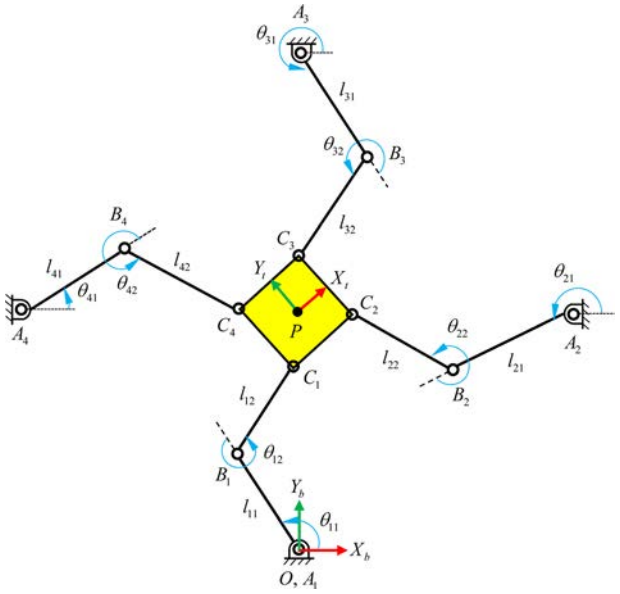

Fig. 4 Schematic diagram of the 4-RRR redundantly actuated manipulator

For each limb, taking the orthogonal product of both sides of Eq. (18) with the general actuation wrench in Eqs. (40) and (41), respectively, yields

$$\begin{aligned}
&\$^r{}_{i_12} \circ \$_P = \$^r{}_{i_12} \circ \$_{i1}\dot{\theta}_{i1} + \$^r{}_{i_12} \circ \$_{i2}\dot{l}_{i1} \quad (i = 1...3)\\
&\$^r{}_{i_123} \circ \$_P = \$^r{}_{i_123} \circ \$_{i1}\dot{\theta}_{i1} + \$^r{}_{i_123} \circ \$_{i2}\dot{l}_{i1}\\
&\qquad + \$^r{}_{i_123} \circ \$_{i3}\dot{\theta}_{i2} \quad (i = 1...3)
\end{aligned} \tag{42}$$

Writing them in matrix form as

$$\boldsymbol{A}_{kf}\dot{\boldsymbol{u}} = \boldsymbol{B}_{kf}\dot{\boldsymbol{\theta}}_{kf} \tag{43}$$

where $\boldsymbol{A}_{kf} \in R^{6\times3}$, $\mathbf{B}_{kf} \in R^{6\times9}$, $\dot{\boldsymbol{\theta}}_{kf} \in R^{9\times1}$

$$\mathbf{A}_{kf} = \begin{bmatrix}
\mathbf{B}_1\mathbf{C}_1 & \hat{z}\cdot(\mathbf{PC}_1 \times \mathbf{B}_1\mathbf{C}_1)\\
\mathbf{B}_1\mathbf{C}_1{}^{\perp} & \hat{z}\cdot(\mathbf{PC}_1 \times \mathbf{B}_1\mathbf{C}_1{}^{\perp})\\
\mathbf{B}_2\mathbf{C}_2 & \hat{z}\cdot(\mathbf{PC}_2 \times \mathbf{B}_2\mathbf{C}_2)\\
\mathbf{B}_2\mathbf{C}_2{}^{\perp} & \hat{z}\cdot(\mathbf{PC}_2 \times \mathbf{B}_2\mathbf{C}_2{}^{\perp})\\
\mathbf{B}_3\mathbf{C}_3 & \hat{z}\cdot(\mathbf{PC}_3 \times \mathbf{B}_3\mathbf{C}_3)\\
\mathbf{B}_3\mathbf{C}_3{}^{\perp} & \hat{z}\cdot(\mathbf{PC}_3 \times \mathbf{B}_3\mathbf{C}_3{}^{\perp})
\end{bmatrix},$$

$$\mathbf{B}_{kf} = \begin{bmatrix}
\xi_{11} & \lambda_{11} & 0 & 0 & 0 & 0 & 0 & 0 & 0\\
\xi_{12} & \lambda_{12} & \beta_{12} & 0 & 0 & 0 & 0 & 0 & 0\\
0 & 0 & 0 & \xi_{21} & \lambda_{21} & 0 & 0 & 0 & 0\\
0 & 0 & 0 & \xi_{22} & \lambda_{22} & \beta_{22} & 0 & 0 & 0\\
0 & 0 & 0 & 0 & 0 & 0 & \xi_{31} & \lambda_{31} & 0\\
0 & 0 & 0 & 0 & 0 & 0 & \xi_{32} & \lambda_{32} & \beta_{32}
\end{bmatrix}$$

$$\xi_{i1} = \$^r{}_{i\_12} \circ \$_{i1}, \quad \lambda_{i1} = \$^r{}_{i\_12} \circ \$_{i2}$$

$$\xi_{i2} = \$^r{}_{i\_123} \circ \$_{i1}, \quad \lambda_{i2} = \$^r{}_{i\_123} \circ \$_{i2}, \quad \beta_{i2} = \$^r{}_{i\_123} \circ \$_{i3}$$

$$\dot{\boldsymbol{u}} = \begin{pmatrix} v_x & v_y & w_z \end{pmatrix}^{\mathrm{T}},$$

$$\dot{\boldsymbol{\theta}}_{kf} = \begin{pmatrix} \dot{\theta}_{11} & \dot{l}_{11} & \dot{\theta}_{12} & \dot{\theta}_{21} & \dot{l}_{21} & \dot{\theta}_{22} & \dot{\theta}_{31} & \dot{l}_{31} & \dot{\theta}_{32} \end{pmatrix}^{\mathrm{T}} \tag{44}$$

As a result, the firstorder kinematics of the 3-RPRR PM with both kinematic and actuation redundancies is expressed in analytical form. It can be found from Eq. (43) that both forward matrix $\boldsymbol{A}_{kf}$ and inverse matrix $\boldsymbol{B}_{kf}$ are nonsquare matrix. Thus, it is not intuitive to find the static force relationship directly from the analytical first-order kinematics. Here, we will introduce how to find the static force relationship of PMs with both kinematic and actuation redundancies. First, from Eq. (43), we can obtain the relationship between independent and dependent joint velocities of the 3-RPRR PM as follows:

$$\boldsymbol{A}_{kf}\dot{\boldsymbol{u}} = \boldsymbol{B}_1\dot{\boldsymbol{\theta}}_a + \boldsymbol{B}_2\dot{\boldsymbol{\theta}}_d \tag{45}$$

where

$$\boldsymbol{B}_1 = \begin{bmatrix}
\xi_{11} & \lambda_{11} & 0 & 0 & 0 & 0\\
\xi_{12} & \lambda_{12} & 0 & 0 & 0 & 0\\
0 & 0 & \xi_{21} & \lambda_{21} & 0 & 0\\
0 & 0 & \xi_{22} & \lambda_{22} & 0 & 0\\
0 & 0 & 0 & 0 & \xi_{31} & \lambda_{31}\\
0 & 0 & 0 & 0 & \xi_{32} & \lambda_{32}
\end{bmatrix} \in R^{6\times6},$$

$$\boldsymbol{B}_2 = \begin{bmatrix}
0 & 0 & 0\\
\beta_{12} & 0 & 0\\
0 & 0 & 0\\
0 & \beta_{22} & 0\\
0 & 0 & 0\\
0 & 0 & \beta_{32}
\end{bmatrix} \in R^{6\times3} \tag{46}$$

$$\dot{\boldsymbol{\theta}}_a = \begin{pmatrix} \dot{\theta}_{11} & \dot{l}_{11} & \dot{\theta}_{21} & \dot{l}_{21} & \dot{\theta}_{31} & \dot{l}_{31} \end{pmatrix}^{\mathrm{T}}$$

$$\dot{\boldsymbol{\theta}}_d = \begin{pmatrix} \dot{\theta}_{12} & \dot{\theta}_{22} & \dot{\theta}_{32} \end{pmatrix}^{\mathrm{T}}$$

It is remarked that even though the PM has actuation redundancy, redundant actuation is just kinematically dependent input. Thus, the motion of the PM can be expressed by the independent input. The relationship between the output velocity vector and independent input velocity vector can be referred to Eq. (22), which can be obtained by taking the orthogonal product of both sides of Eq. (18) with the general actuation wrench of Eq. (40).

Inserting the forward kinematics of the PM expressed by Eq. (22) into Eq. (45), we have

$$\begin{aligned}
&\boldsymbol{A}_{kf}\dot{\boldsymbol{u}} = \boldsymbol{A}_{kf}\boldsymbol{J}\dot{\boldsymbol{\theta}}_a = \boldsymbol{B}_1\dot{\boldsymbol{\theta}}_a + \boldsymbol{B}_2\dot{\boldsymbol{\theta}}_d\\
&\boldsymbol{B}_2\dot{\boldsymbol{\theta}}_d = (\boldsymbol{A}_{kf}\boldsymbol{J} - \boldsymbol{B}_1)\dot{\boldsymbol{\theta}}_a
\end{aligned} \tag{47}$$

Due to the fact that dependent joint velocities $\dot{\boldsymbol{\theta}}_d$ can be expressed in terms of independent joint velocities $\dot{\boldsymbol{\theta}}_a$ uniquely, from Eq. (47), we have

$$\dot{\boldsymbol{\theta}}_d = \boldsymbol{B}_2^{+}(\boldsymbol{A}_{kf}\boldsymbol{J} - \boldsymbol{B}_1)\dot{\boldsymbol{\theta}}_a = \left[\boldsymbol{G}_a^d\right]\dot{\boldsymbol{\theta}}_a \tag{48}$$

where $\boldsymbol{B}_2^{+} = (\boldsymbol{B}_2{}^{\mathrm{T}}\boldsymbol{B}_2)^{-1}\boldsymbol{B}_2{}^{\mathrm{T}}$ denoting the left-pseudo inverse of $\boldsymbol{B}_2$ has a unique solution because of geometrically compatible characteristic of the PM.

In order to maintain the static equilibrium against external force $\boldsymbol{F}$, using the virtual work principle, we have

$$\boldsymbol{F}^{\mathrm{T}}\delta\boldsymbol{u} = \boldsymbol{\tau}_{kf}{}^{\mathrm{T}}\delta\boldsymbol{\theta}_{kf} \tag{49}$$

where $\boldsymbol{\tau}_{kf} = \begin{bmatrix} \boldsymbol{\tau}_a \\ \boldsymbol{\tau}_d \end{bmatrix} = (\tau_{11}\ f_{11}\ \tau_{21}\ f_{21}\ \tau_{31}\ f_{31}\ \tau_{12}\ \tau_{22}\ \tau_{32})^{\mathrm{T}} \in R^{9\times1}$,

$\delta\boldsymbol{\theta}_{kf} = \begin{bmatrix} \delta\boldsymbol{\theta}_a \\ \delta\boldsymbol{\theta}_d \end{bmatrix}$.

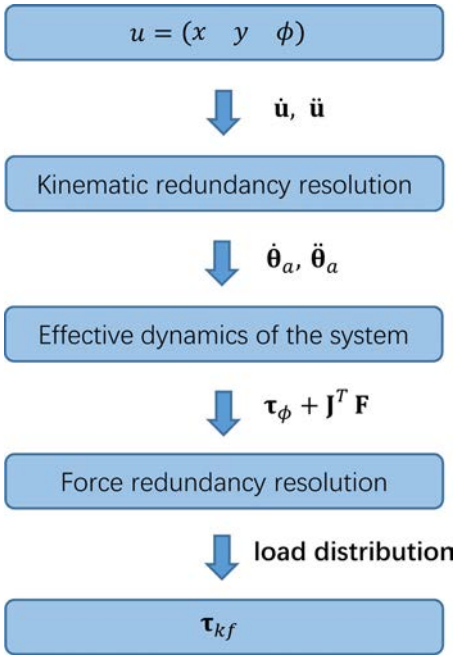

Fig. 5 Flowchart of the hybrid resolution algorithm

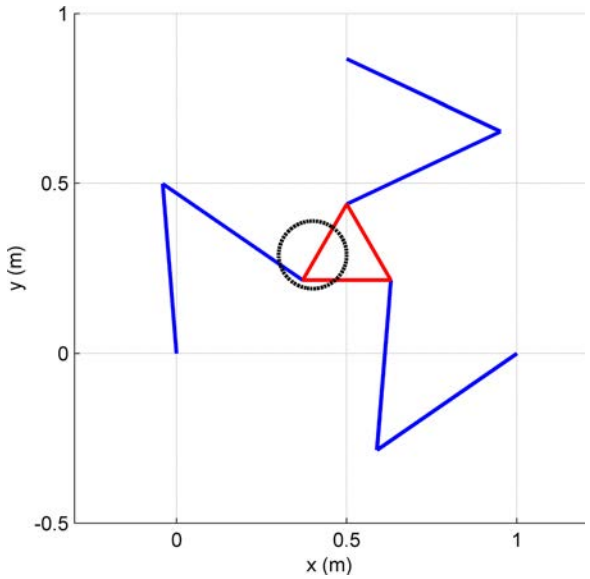

Fig. 6 Desired trajectory and initial configuration

From Eqs. (22) and (48), we have

$$\delta \boldsymbol{u} = \boldsymbol{J}\delta\boldsymbol{\theta}_a, \quad \delta\boldsymbol{\theta}_{kf} = \begin{bmatrix} \delta\boldsymbol{\theta}_a \\ \delta\boldsymbol{\theta}_d \end{bmatrix} = \begin{bmatrix} \boldsymbol{I}_{6\times 6} \\ [\boldsymbol{G}_a^d] \end{bmatrix} \delta\boldsymbol{\theta}_a \tag{50}$$

Combining Eq. (49) with Eq. (50), we have

$$\boldsymbol{F}^{\mathrm{T}}\boldsymbol{J}\delta\boldsymbol{\theta}_a = {\boldsymbol{\tau}_{kf}}^{\mathrm{T}} \begin{bmatrix} \boldsymbol{I}_{6\times 6} \\ [\boldsymbol{G}_a^d] \end{bmatrix} \delta\boldsymbol{\theta}_a \tag{51}$$

Finally, the static force relationship can be expressed as

$$\boldsymbol{J}^{\mathrm{T}}\boldsymbol{F} = \boldsymbol{J}_{kp}\boldsymbol{\tau}_{kf} \tag{52}$$

where $\boldsymbol{J}_{kp} = \begin{bmatrix} \boldsymbol{I}_{6\times 6} & [\boldsymbol{G}_a^d]^{\mathrm{T}} \end{bmatrix} \in R^{6\times 9}$.

The general solution of Eq. (52) is given as

$$\boldsymbol{\tau}_{kf} = {\boldsymbol{J}_{kp}}^{+}(\boldsymbol{J}^{\mathrm{T}}\boldsymbol{F}) + (\boldsymbol{I} - {\boldsymbol{J}_{kp}}^{+}\boldsymbol{J}_{kp})\boldsymbol{\varepsilon} \tag{53}$$

where ${\boldsymbol{J}_{kp}}^{+}$ is the pseudoinverse of $\boldsymbol{J}_{kp}$, $\boldsymbol{I} \in R^{9\times 9}$ is an identity matrix, and $\boldsymbol{\varepsilon} \in R^9$ is an arbitrary vector.

As a result, the static force relationship of the 3-RPRR PM with both kinematic and actuation redundancies is obtained in analytical form. Together with the first-order kinematics in Eq. (43), we can conclude that for PMs with both kinematic and actuation redundancies

(1) Give $\dot{\boldsymbol{u}}$, there exists infinite number of $\dot{\boldsymbol{\theta}}_{kf}$, which implies the redundancy resolution in kinematic level. (23)
(2) Give $\boldsymbol{F}$, there exists infinite number of $\boldsymbol{\tau}_{kf}$, which implies the redundancy resolution in force level. (53)

Thus, a hybrid resolution algorithm is required to control this kind of PMs with both kinematic and actuation redundancies. Without loss of generality, let us consider the case that the manipulator is moving by following some specified trajectory path together with the task to exert some external force $\boldsymbol{F}$ on the environment. The flowchart in Fig. 5 illustrates the hybrid resolution algorithm proposed. Degrees of the kinematic redundancies and actuation redundancies can be utilized to reconfigure the limb for specified task position and distribute the load of the total system, respectively. This hybrid resolution algorithm can be applied to motion generation of the system with both kinematic and actuation redundancies. Even though control of this kind of PMs is comparatively complex, it inherently features with the advantages of PMs with pure kinematic redundancy and pure actuation redundancy simultaneously.

From the above four example PMs, we clearly demonstrate how to develop the Jacobian of PMs with different types of redundancies by using the screw theory. Comparison of Jacobian for these four examples is illustrated in Table 2 conclusively.

4 Simulations

In this section, some simulations are performed to demonstrate that kinematic redundancy and actuation redundancy can be utilized to improve the performance of PMs. The same desired trajectory together with the task to exert some external force $\boldsymbol{F}$ on the environment is specified for the performance comparison. In Fig. 1, geometric parameters of the 3-RRR chain are assumed to be

$$l_{i1} = l_{i2} = 0.5\,m,\ PC_i = 0.15\,m,\ A_iA_j = 1.0\,m\,(i \neq j),\ i, j = 1, 2, 3$$

Geometric parameters of the RPRR and RPRR chains of Figs. 2 and 3 are given as

$$0.1\,\mathrm{m} \leq l_{i1} \leq 0.9\,\mathrm{m},\ l_{i2} = 0.5\,m,\ PC_i = 0.15\,m,\ A_iA_j = 1.0\,m\,(i \neq j),\ i, j = 1, 2, 3$$

Table 2 Jacobian comparison of the example mechanisms

Architecture	Redundancy classification	First-order kinematics	Dimension of the forward and inverse matrices	Static force relationship
3-RRR[a]	No redundancy	$\mathbf{A}\dot{u} = \mathbf{B}\dot{\boldsymbol{\theta}}_a$	$\mathbf{A} \in R^{3\times 3},\ \mathbf{B} \in R^{3\times 3}$ $\dot{\mathbf{u}} \in R^{3\times 1},\ \dot{\boldsymbol{\theta}}_a \in R^{3\times 1}$	$\boldsymbol{\tau}_a = (\mathbf{A}^{-1}\mathbf{B})^T\mathbf{F}$
3-RPRR	Kinematic redundancy	$\mathbf{A}\dot{u} = \mathbf{B}\dot{\boldsymbol{\theta}}_a$	$\mathbf{A} \in R^{3\times 3},\ \mathbf{B} \in R^{3\times 6}$ $\dot{\mathbf{u}} \in R^{3\times 1},\ \dot{\boldsymbol{\theta}}_a \in R^{6\times 1}$	$\boldsymbol{\tau}_a = (\mathbf{A}^{-1}\mathbf{B})^T\mathbf{F}$
RRR-RPRR-RPRRR	Kinematic redundancy	$\mathbf{A}\dot{u} = \mathbf{B}\dot{\boldsymbol{\theta}}_a$	$\mathbf{A} \in R^{3\times 3},\ \mathbf{B} \in R^{3\times 6}$ $\dot{\mathbf{u}} \in R^{3\times 1},\ \dot{\boldsymbol{\theta}}_a \in R^{6\times 1}$	$\boldsymbol{\tau}_a = (\mathbf{A}^{-1}\mathbf{B})^T\mathbf{F}$
4-RRR	Actuation redundancy	$\mathbf{A}\dot{u} = \mathbf{B}\dot{\boldsymbol{\theta}}_a$	$\mathbf{A} \in R^{4\times 3},\ \mathbf{B} \in R^{4\times 4}$ $\dot{\mathbf{u}} \in R^{3\times 1},\ \dot{\boldsymbol{\theta}}_a \in R^{4\times 1}$	$\mathbf{F} = (\mathbf{B}^{-1}\mathbf{A})^T\boldsymbol{\tau}_a$
3-RPRR	Kinematic and actuation redundancies	$\mathbf{A}\dot{u} = \mathbf{B}\dot{\boldsymbol{\theta}}_{kf}$	$\mathbf{A}_{kf} \in R^{6\times 3},\ \mathbf{B}_{kf} \in R^{6\times 9}$ $\dot{\mathbf{u}} \in R^{3\times 1},\ \dot{\boldsymbol{\theta}}_{kf} \in R^{9\times 1}$	$\mathbf{J}_{kp}\boldsymbol{\tau}_{kf} = \mathbf{J}^T\mathbf{F} \rightarrow$ $\boldsymbol{\tau}_{kf} = (\mathbf{J}_{kp})^{+}\mathbf{J}^T\mathbf{F}$ $\mathbf{J}_{kp} \in R^{6\times 9},\ \mathbf{J} \in R^{3\times 6}$

[a]Under-bar implies the actuated joint

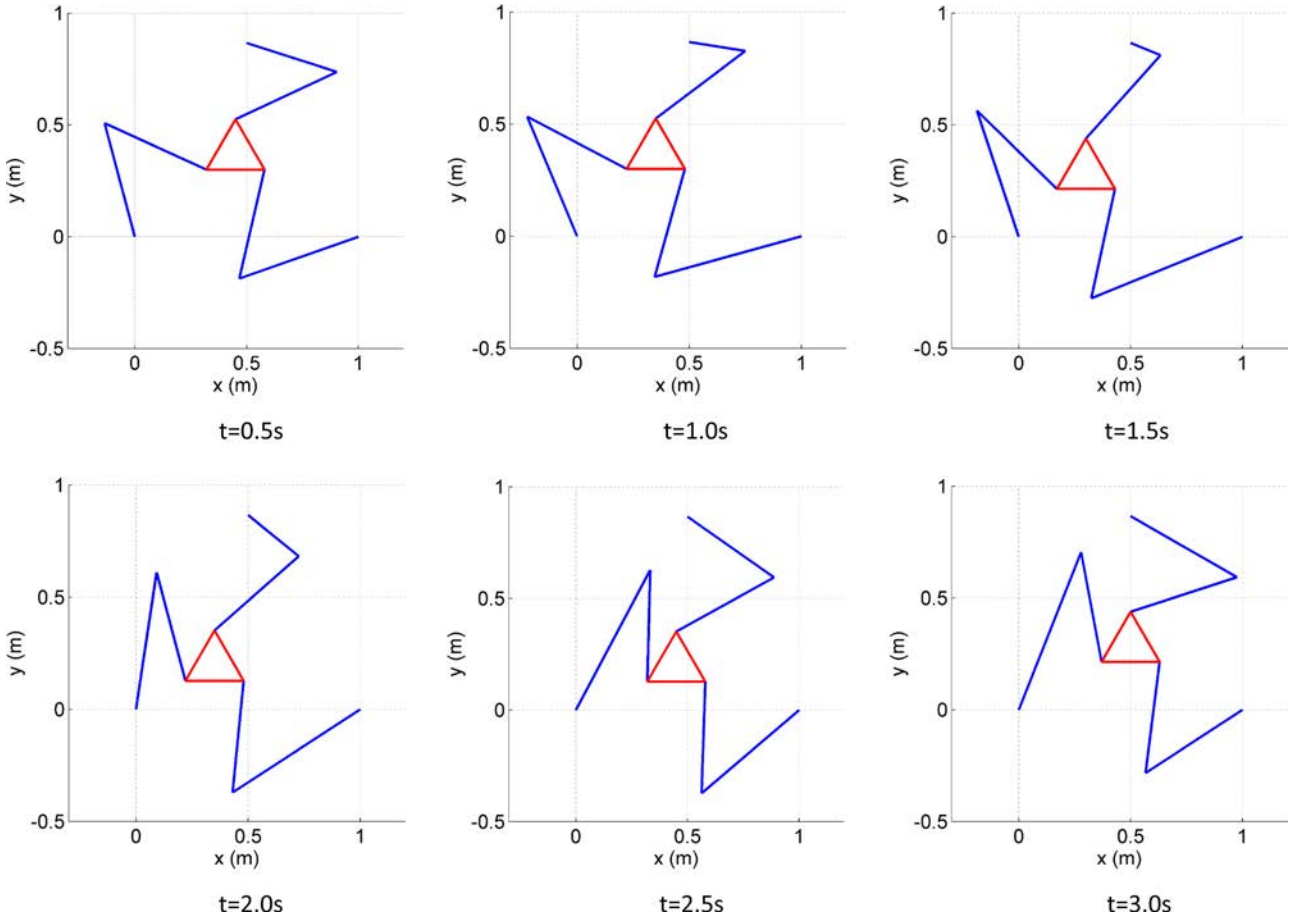

Fig. 7 Joint configurations during the trajectory: case of minimum norm solution

The same desired trajectory (a circle in 3 s) is defined as

$$x = L/2 - r + r\cos((2\pi/3)t)$$
$$y = \sqrt{3}L/6 + r\sin((2\pi/3)t)$$
$$\phi_z = 0$$

where $L = A_iA_j\ (i \neq j),\ \ r = 0.1\,m$.

Figure 6 shows the initial configuration and desired trajectory (a circle represented by the dashed line). For kinematic redundant 3-RPRR PM, when specifying the desired output trajectory, input joint displacements can be found as $\dot{\boldsymbol{\theta}}_a = \boldsymbol{J}^{+}\dot{\boldsymbol{u}} + (\boldsymbol{I} - \boldsymbol{J}^{+}\boldsymbol{J})\boldsymbol{\varepsilon}$, where $\boldsymbol{J}^{+} = \boldsymbol{J}^{\mathrm{T}}(\boldsymbol{J}\boldsymbol{J}^{\mathrm{T}})^{-1}$. The first part implies the minimum norm solution, and second part implies the null space solution.

Figures 7 and 8 illustrate the joint configurations and link length variations of three redundant prismatic joints of the minimum norm solution during the trajectory, respectively. As we know, type II singularities will happen when $\det(\boldsymbol{A}) = 0$. Here, we want to maximize $\sqrt{\det(\boldsymbol{A}\boldsymbol{A}^{\mathrm{T}})}$ with the help of the null space solution. Potential function is defined as $p(\boldsymbol{\theta}_a) = -\sqrt{\det(\boldsymbol{A}\boldsymbol{A}^{\mathrm{T}})}$. To minimize the potential function, input joint displacements is found as $\dot{\boldsymbol{\theta}}_a = \boldsymbol{J}^{\mathrm{T}}(\boldsymbol{J}\boldsymbol{J}^{\mathrm{T}})^{-1}\dot{\boldsymbol{u}} + \left(\boldsymbol{I} - \boldsymbol{J}^{\mathrm{T}}(\boldsymbol{J}\boldsymbol{J}^{\mathrm{T}})^{-1}\boldsymbol{J}\right)\left(-k\dfrac{\partial p}{\partial \boldsymbol{\theta}_a}\right)^{\mathrm{T}}$.

Figures 9 and 10 illustrate the joint configurations and link length variations of three redundant prismatic joints of the optimized null-space solution during the trajectory, respectively. Figure 11 clearly demonstrates that kinematic redundancy can be utilized to avoid type II singularities (maximize the $\sqrt{\det(\boldsymbol{A}\boldsymbol{A}^{\mathrm{T}})}$) by comparing the optimized null space solution with the minimum norm solution.

Moreover, in order to withstand the external force $\boldsymbol{F} = \begin{pmatrix} 2\,\mathrm{N} & 2\,\mathrm{N} & 0.2\,\mathrm{N}\cdot\mathrm{m} \end{pmatrix}$ during the desired trajectory, comparison of Euclidean norm of the actuation torque of 3-RPRR PM with that of 3-RPRR PM required is illustrated in Fig. 12. Here, for 3-RPRR PM with both kinematic and actuation redundancies,

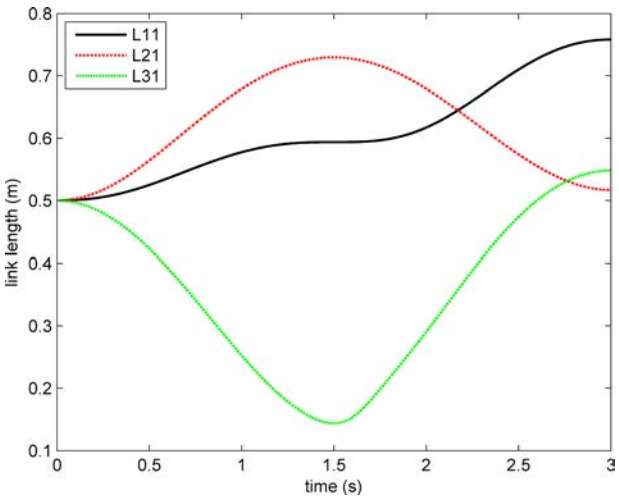

Fig. 8 Link length variations of the three redundant prismatic joints: case of minimum norm solution

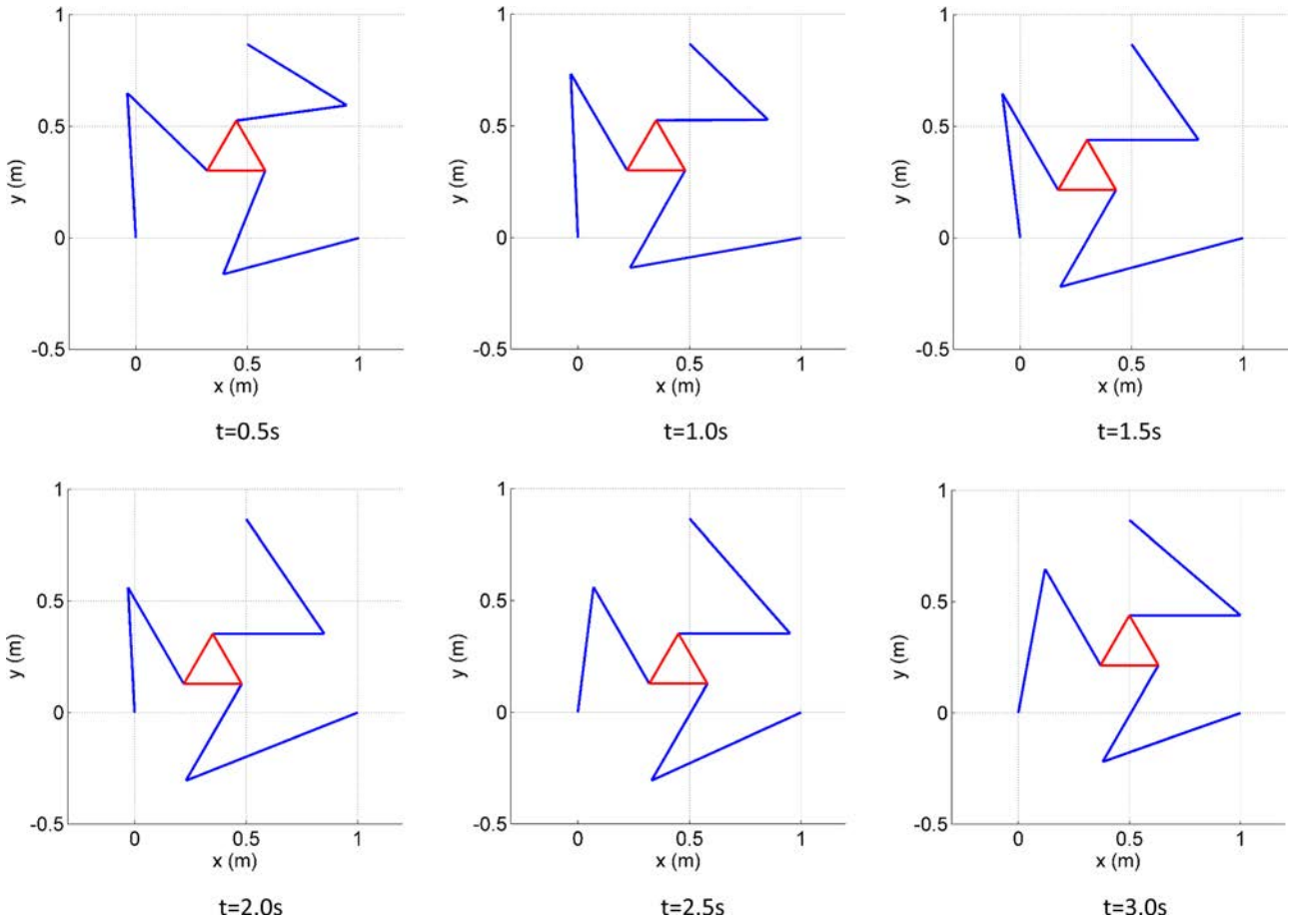

Fig. 9 Joint configurations during the trajectory: case of optimized null-space solution

the minimum norm solution $\boldsymbol{\tau}_{kf} = (\boldsymbol{J}_{kp})^{+}\boldsymbol{J}^{\mathrm{T}}\boldsymbol{F}$ with $(\boldsymbol{J}_{kp})^{+} = \boldsymbol{J}_{kp}^{\mathrm{T}}\left(\boldsymbol{J}_{kp}\boldsymbol{J}_{kp}^{\mathrm{T}}\right)^{-1}$ is utilized for comparison. It is noted from Fig. 12 that redundant actuation greatly reduces the actuation effort of the whole system. In other words, multiple less powerful actuators can be utilized in the PM with both kinematic and actuation redundancies instead of using powerful actuators in the PM with only kinematic redundancy.

5 Conclusions

For PMs with kinematic redundancy, screw theory has not been attempted to develop the analytical Jacobian matrix to the best of our knowledge. By extending the screw theory to PMs with kinematic redundancy, a general formulation to obtain the analytical Jacobian of arbitrary conventional PMs was developed. The method was successfully applied to a simple planar example and its variations with kinematic and actuation redundancies. Moreover, we focused on PMs with both kinematic and actuation redundancies to show how to derive the first-order kinematics and

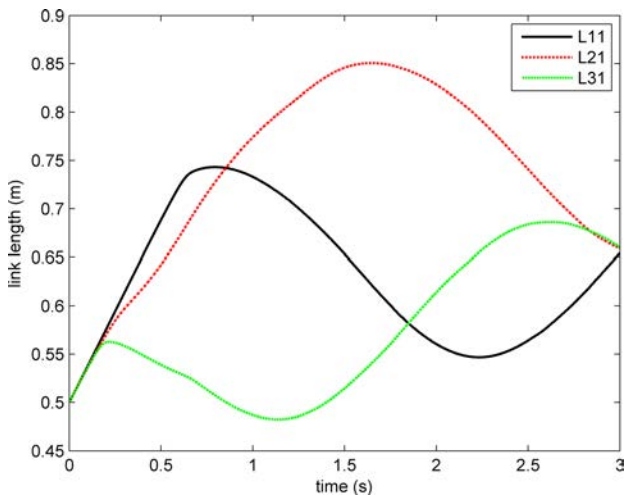

Fig. 10 Link length variations of the three redundant prismatic joints: case of optimized null-space solution

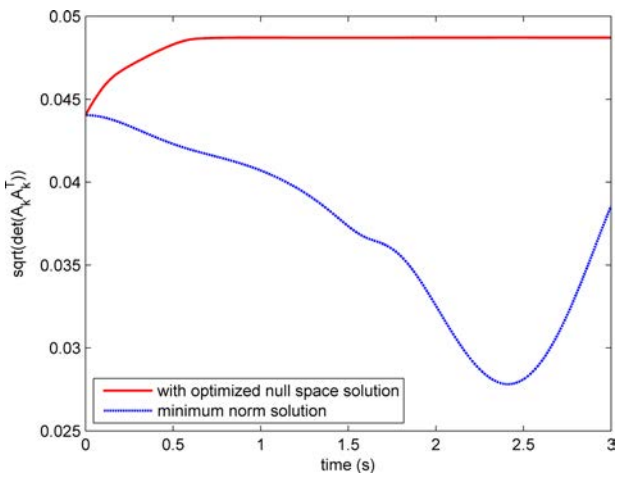

Fig. 11 Variations of $\sqrt{\det(AA^{\mathrm{T}})}$ for two different inverse kinematic solutions of 3-RPRR PM

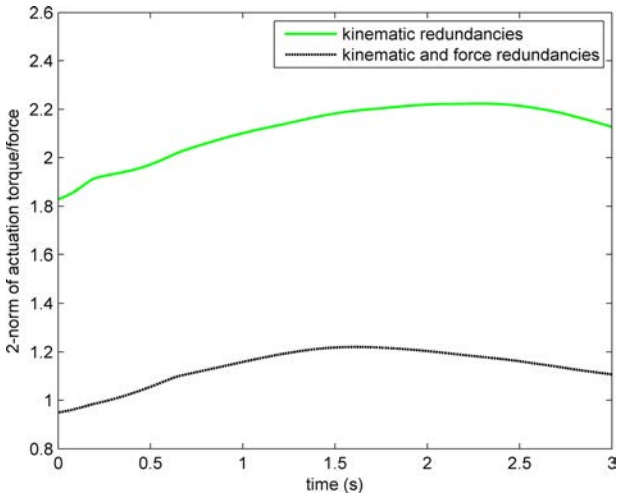

Fig. 12 Comparison of 2-norm of the actuation torque/force of the 3-RPRR PM with that of the 3-RPRR PM

the static force relationship in analytical form. Some simulations were performed to demonstrate the advantages of kinematic and actuation redundancies. Through the analytical Jacobian, we found that the kinematic redundancy resolution can be employed for the given posture. Similarly, actuation redundancy resolution can be employed for the given external wrench. Thus, to control this kind of PMs, a hybrid resolution algorithm considering both kinematic and actuation redundancy resolution level is required, and one example algorithm is proposed. Through the above analysis, it is believed that PMs with both kinematic and actuation redundancies would possess potential advantages which are introduced by the kinematic redundancy and actuation redundancy simultaneously. Future work includes suggesting more hybrid resolution algorithms for practical implementation and new performance indices, such as motion/force transmissibility [45], for optimal design of PMs with both kinematic and actuation redundancies.

Acknowledgment

This work was supported by the Technology Innovation Program (10052980, Development of microrobotic system for surgical treatment of chronic total occlusion) funded by the Ministry of Trade, Industry & Energy (MOTIE, Korea). This work performed by ICT based Medical Robotic Systems Team of Hanyang University, Department of Electronic Systems Engineering was supported by the BK21 Plus Program funded by National Research Foundation of Korea (NRF), and supported by WC300 R&D Program (S2482672) funded by the Small and Medium Business Administration (SMBA, Korea).

References

[1] Maciejewski, A. A., and Klein, C. A., 1985, "Obstacle Avoidance for Kinematically Redundant Manipulators in Dynamically Varying Environments," Int. J. Rob. Res., **4**(3), pp. 109–117.
[2] Wang, J., and Gosselin, C. M., 2004, "Kinematic Analysis and Design of Kinematically Redundant Parallel Mechanisms," ASME J. Mech. Des., **126**(1), pp. 109–118.
[3] Ebrahimi, I., Carretero, J. A., and Boudreau, R., 2007, "3-PRRR Redundant Planar Parallel Manipulator: Inverse Displacement, Workspace and Singularity Analyses," Mech. Mach. Theory, **42**(8), pp. 1007–1016.
[4] Gosselin, C. M., Laliberté, T., and Veillette, A., 2015, "Singularity-Free Kinematically Redundant Planar Parallel Mechanisms With Unlimited Rotational Capability," IEEE Trans. Rob., **31**(2), pp. 457–467.
[5] Shimizu, M., Yoon, W. K., and Kitagaki, K., "A Practical Redundancy Resolution for 7 DOF Redundant Manipulators With Joint Limits," IEEE International Conference on Robotics and Automation (ICRA), Rome, Italy, Apr. 10–14, pp. 4510–4516.
[6] Flacco, F., Luca, A. D., and Khatib, O., "Motion Control of Redundant Robots Under Joint Constraints: Saturation in the Null Space," IEEE International Conference on Robotics and Automation (ICRA), Saint Paul, MN, May 14–18, pp. 285–292.
[7] Hollerbach, J., and Ki, S., 1987, "Redundancy Resolution of Manipulators Through Torque Optimization," IEEE J. Rob. Autom., **3**(4), pp. 308–316.
[8] Chiaverini, S., 1997, "Singularity-Robust Task-Priority Redundancy Resolution for Real-Time Kinematic Control of Robot Manipulators," IEEE Trans. Rob. Autom., **13**(3), pp. 398–410.
[9] Klein, C. A., and Blaho, B. E., 1987, "Dexterity Measures for the Design and Control of Kinematically Redundant Manipulators," Int. J. Rob. Res., **6**(2), pp. 72–83.
[10] Nakamura, Y., 1991, *Advanced Robotics: Redundancy and Optimization*, Addison-Wesley, Boston, MA.
[11] Yi, B.-J., Na, H. Y., Lee, J. H., Hong, Y.-S., Oh, S.-R., Suh, I. H., and Kim, W. K., 2002, "Design of a Parallel-Type Gripper Mechanism," Int. J. Rob. Res., **21**(7), pp. 661–676.
[12] Mohamed, M. G., and Gosselin, C. M., 2005, "Design and Analysis of Kinematically Redundant Parallel Manipulators With Configurable Platforms," IEEE Trans. Rob., **21**(3), pp. 277–287.
[13] Isaksson, M., Gosselin, C., and Marlow, K., 2016, "An Introduction to Utilising the Redundancy of a Kinematically Redundant Parallel Manipulator to Operate a Gripper," Mech. Mach. Theory, **101**, pp. 50–59.
[14] Saglia, J. A., Dai, J. S., and Caldwell, D. G., 2008, "Geometry and Kinematic Analysis of a Redundantly Actuated Parallel Mechanism That Eliminates Singularities and Improves Dexterity," ASME J. Mech. Des., **130**(12), p. 124501.
[15] Shayya, S., Krut, S., Company, O., Baradat, C., and Pierrot, F., 2013, "A Novel (3T-1R) Redundant Parallel Mechanism With Large Operational Workspace and Rotational Capability," IEEE/RSJ International Conference on Intelligent Robots and Systems (IROS), Tokyo, Japan, Nov. 3–7, pp. 436–443.
[16] Shin, H., Lee, S., Jeong, J. I., and Kim, J., 2013, "Antagonistic Stiffness Optimization of Redundantly Actuated Parallel Manipulators in a Predefined Workspace," IEEE/ASME Trans. Mechatronics, **18**(3), pp. 1161–1169.
[17] Wang, C., Fang, Y., Guo, S., and Chen, Y., 2013, "Design and Kinematical Performance Analysis of a 3-RUS/RRR Redundantly Actuated Parallel Mechanism for Ankle Rehabilitation," ASME J. Mech. Rob., **5**(4), p. 041003.
[18] Corbel, D., Gouttefarde, M., Company, O., and Pierrot, F., 2010, "Actuation Redundancy as a Way to Improve the Acceleration Capabilities of 3T and 3T1R Pick-and-Place Parallel Manipulators," ASME J. Mech. Rob., **2**(4), p. 041002.
[19] Li, Q., Zhang, N., and Wang, F., 2016, "New Indices for Optimal Design of Redundantly Actuated Parallel Manipulators," ASME J. Mech. Rob., **9**(1), p. 011007.
[20] Kang, L., Kim, W., and Yi, B. J., 2016, "Kinematic Modeling, Analysis, and Load Distribution Algorithm for a Redundantly Actuated 4-DOF Parallel Mechanism," IEEE/RSJ International Conference on Intelligent Robots and Systems (IROS), Daejeon, South Korea, Oct. 9–14, pp. 356–361.
[21] Yung, T., Tosunoglu, S., and Freeman, R., 1993, "Actuator Saturation Avoidance for Fault-Tolerant Robots," 32nd IEEE Conference on Decision and Control (CDC), San Antonio, TX, Dec. 15–17, pp. 2125–2130.
[22] Gouttefarde, M., Daney, D., and Merlet, J. P., 2011, "Interval-Analysis-Based Determination of the Wrench-Feasible Workspace of Parallel Cable-Driven Robots," IEEE Trans. Rob., **27**(1), pp. 1–13.
[23] Gosselin, C., and Grenier, M., 2011, "On the Determination of the Force Distribution in Overconstrained Cable-Driven Parallel Mechanisms," Meccanica, **46**(1), pp. 3–15.
[24] Bouchard, S., Gosselin, C., and Moore, B., 2009, "On the Ability of a Cable-Driven Robot to Generate a Prescribed Set of Wrenches," ASME J. Mech. Rob., **2**(1), p. 011010.
[25] Hassan, M., and Khajepour, A., 2008, "Optimization of Actuator Forces in Cable-Based Parallel Manipulators Using Convex Analysis," IEEE Trans. Rob., **24**(3), pp. 736–740.
[26] Yuan, H., Courteille, E., and Deblaise, D., 2016, "Force Distribution With Pose-Dependent Force Boundaries for Redundantly Actuated Cable-Driven Parallel Robots," ASME J. Mech. Rob., **8**(4), p. 041004.
[27] Davies, T. H., 1981, "Kirchhoff's Circulation Law Applied to Multi-Loop Kinematic Chains," Mech. Mach. Theory, **16**(3), pp. 171–183.
[28] Mohamed, M. G., and Duffy, J., 1985, "A Direct Determination of the Instantaneous Kinematics of Fully Parallel Robot Manipulators," ASME. J. Mech., Transm., Autom. Des., **107**(2), pp. 226–229.
[29] Joshi, S. A., and Tsai, L.-W., 2002, "Jacobian Analysis of Limited-DOF Parallel Manipulators," ASME J. Mech. Des., **124**(2), pp. 254–258.
[30] Cox, D. J., 1981, "The Dynamic Modeling and Command Signal Formulation for Parallel Multi-Parameter Robotic Devices," Master's thesis, University of Florida, Gainesville, FL.
[31] Cox, D. J., and Tesar, D., 1989, "The Dynamic Model of a Three Degree of Freedom Parallel Robotic Shoulder Module," *Advanced Robotics: Proceedings of the 4th International Conference on Advanced Robotics*, K. J. Waldron, ed., Springer, Berlin, pp. 475–487.
[32] Yi, B.-J., Kim, S. M., Kwak, H. K., and Kim, W., 2013, "Multi-Task Oriented Design of an Asymmetric 3T1R Type 4-DOF Parallel Mechanism," Proc. Inst Mech Eng. Part C, **227**(10), pp. 2236–2255.
[33] Kang, L., and Yi, B. J., 2016, "Design of Two Foldable Mechanisms Without Parasitic Motion," IEEE Robot. Autom. Lett., **1**(2), pp. 930–937.
[34] Isaksson, M., Gosselin, C., and Marlow, K., 2017, "Singularity Analysis of a Class of Kinematically Redundant Parallel Schönflies Motion Generators," Mech. Mach. Theory, **112**, pp. 172–191.
[35] Isaksson, M., 2017, "Kinematically Redundant Planar Parallel Mechanisms for Optimal Singularity Avoidance," ASME J. Mech. Des., **139**(4), p. 042302.
[36] Gogu, G., 2005, "Mobility of Mechanisms: A Critical Review," Mech. Mach. Theory, **40**(9), pp. 1068–1097.
[37] Li, Q. C., and Huang, Z., 2004, "Mobility Analysis of a Novel 3-5R Parallel Mechanism Family," ASME J. Mech. Des., **126**(1), pp. 79–82.

[38] Dai, J. S., Huang, Z., and Lipkin, H., 2004, "Mobility of Overconstrained Parallel Mechanisms," ASME J. Mech. Des., **128**(1), pp. 220–229.
[39] Zanchettin, A. M., Rocco, P., Robertsson, A., and Johansson, R., 2011, "Exploiting Task Redundancy in Industrial Manipulators During Drilling Operations," IEEE International Conference on Robotics and Automation (ICRA), Shanghai, China, May 9–13, pp. 128–133.
[40] Nokleby, S. B., Fisher, R., Podhorodeski, R. P., and Firmani, F., 2005, "Force Capabilities of Redundantly-Actuated Parallel Manipulators," Mech. Mach. Theory, **40**(5), pp. 578–599.
[41] Gosselin, C., and Angeles, J., 1988, "The Optimum Kinematic Design of a Planar Three-Degree-of-Freedom Parallel Manipulator," ASME. J. Mech., Transm., Autom. Des., **110**(1), pp. 35–41.
[42] Bonev, I. A., Zlatanov, D., and Gosselin, C. M. M., 2003, "Singularity Analysis of 3-DOF Planar Parallel Mechanisms Via Screw Theory," ASME J. Mech. Des., **125**(3), pp. 573–581.
[43] Huang, T., Liu, H. T., and Chetwynd, D. G., 2011, "Generalized Jacobian Analysis of Lower Mobility Manipulators," Mech. Mach. Theory, **46**(6), pp. 831–844.
[44] Cha, S. H., Lasky, T. A., and Velinsky, S. A., 2007, "Singularity Avoidance for the 3-RRR Mechanism Using Kinematic Redundancy," IEEE International Conference on Robotics and Automation (ICRA), Rome, Italy, Apr. 10–14, pp. 1195–1200.
[45] Chen, X., Chen, C., and Liu, X.-J., 2015, "Evaluation of Force/Torque Transmission Quality for Parallel Manipulators," ASME J. Mech. Rob., **7**(4), p. 041013.